RESEARCH ARTICLE | AUGUST 12 2019

Electrochromic properties of $Li_4Ti_5O_{12}$: From visible to infrared spectrum

Meng Li; Tim Gould; Zhong Su; Shunning Li; Feng Pan; Shanqing Zhang

Appl. Phys. Lett. 115, 073902 (2019)
https://doi.org/10.1063/1.5099330

Applied Physics Letters ARTICLE scitation.org/journal/apl

Electrochromic properties of $Li_4Ti_5O_{12}$: From visible to infrared spectrum

Cite as: Appl. Phys. Lett. **115**, 073902 (2019); doi: 10.1063/1.5099330
Submitted: 9 April 2019 · Accepted: 8 July 2019 ·
Published Online: 12 August 2019

Meng Li,[1,2,3] Tim Gould,[3,a)] Zhong Su,[1] Shunning Li,[2] Feng Pan,[2,b)] and Shanqing Zhang[1,c)]

AFFILIATIONS

[1]Centre for Clean Environment and Energy, and School of Environment and Science, Gold Coast Campus, Griffith University, Gold Coast, QLD 4222, Australia
[2]School of Advanced Materials, Shenzhen Graduate School, Peking University, Shenzhen 518055, China
[3]Queensland Micro- and Nanotechnology Centre, Nathan Campus, Griffith University, Brisbane, QLD 4111, Australia

[a)]Electronic mail: t.gould@griffith.edu.au
[b)]Electronic mail: panfeng@pkusz.edu.cn
[c)]Electronic mail: s.zhang@griffith.edu.au

ABSTRACT

Recently, $Li_4Ti_5O_{12}$ (LTO) has been experimentally proven as a promising broadband electrochromic material for applications like smart windows, thermal management, and infrared camouflage. However, a detailed understanding of the fundamental mechanism of these phenomena is still lacking, especially how and why the optical spectrum changes with lithiation. We fill this knowledge gap by performing a detailed analysis of LTO's optical properties during charging/discharging via a robust study of the density functional theory (DFT). Our study suggests that the absorption of infrared light is highly sensitive to intercalation of Li in the LTO lattice, in contrast to that of visible wavelengths. This unique characteristic of LTO offers an effective mechanism in controlling infrared radiation intensity with minimal attenuation on the transmission of visible light. Furthermore, the DFT study also reveals that the electrochemical intercalation of Li introduces donor states which will gradually expand and move to deeper levels in the forbidden band. This electronic structure change leads to better conductivity and lower transmittance, which is in line with the experimental observation in the literature.

Electrochromism is a phenomenon related to the reversible changes in optical properties (e.g., absorbance, reflectance, and transmittance) of a material induced by externally applied potentials. Since the pioneering work by Deb using tungsten oxide films in 1969,[1] electrochromic materials are gradually attracting significant attention in academia and industry.[2,3] Traditional studies focus on color changes in the visible region, which find broad potential and practical applications such as auto-dimming rearview mirrors and smart windows. The latter is a major application area due to the popularity of large window panes in modern buildings. The active layer of an electrochromic panel is typically a two-electrode electrochemical system which is sealed and isolated from an ambient environment. Smart glass can meet the design aspirations of comfortable illumination, being able to increase or reduce light transmission, which makes them very attractive for saving electric energy, especially in view of global warming. Over the last decade, increasing interest has been shifting to the infrared (IR) region, which could be exploitable for infrared camouflage, data storage, optical communication, and thermal management in buildings and spacecraft.[4–8]

After decades of active research, the vast majority of materials used in the field of electrochromism are either conductive polymers, cyanometallates (e.g., Prussian Blue), or transition metal oxides.[2] The metal oxides have been extensively studied due to their remarkable long-term and high-temperature stability. $Li_4Ti_5O_{12}$ (LTO), which is a promising anode material because of its notable "zero-strain" characteristic,[9] was first observed to change color under applied voltage in 2010.[10] Last year, Mandal *et al.*[11] reported its electrochromic properties in the infrared region. The broadband electrochromic properties, large tunability, and excellent thermal stability give LTO attractive potential in a wide range of applications.

However, understanding of the mechanisms responsible for LTO's electrochromism is still lacking. For example, Mandal *et al.* argued that $Li_4Ti_5O_{12}$ (bleached state) has a high reflectance when nanostructured, compared to $Li_{12}Ti_5O_{12}$ (colored state). But this explanation violates the general rule that, the better the conductivity, the higher the reflectivity; this high reflectivity is mainly contributed to the substrate material (Al), which is coated by a low absorbance material ($Li_4Ti_5O_{12}$). This result highlights the difficulty of obtaining

accurate results in experiments, which will be affected by instruments, test methods, surroundings, and many other factors. Computational and theoretical investigation is urgently needed to supplement and explain the experiments due to its ability to control such factors and to provide direct insights into electronic structure and related properties, i.e., quantitative relationship between the spectrum and the degree of lithiation.

Some basic properties of LTO remain unknown: (i) detailed optical properties have not been calculated, particularly in the infrared region; (ii) the corresponding electronic structure of LTO has not been quantitatively investigated during the charging/discharging process; (iii) the electronic structure-property relationship has not been discussed or analyzed. That is, the underlying mechanism of its electrochromism has not been made clear. Therefore, to fill these gaps, the present work reports the optical and electronic properties of LTO obtained by density functional theory (DFT). Our results thus help interpret and refine previous experimental conclusions and offer insights into the electrochromic properties of LTO.

The rest of this manuscript proceeds as follows: First, we summarize the materials and calculation method. Next, we explain the electrochromic mechanism of LTO via electronic properties. Then, we analyze the optical properties of LTO with and without intercalated Li. Finally, we discuss applications of LTO and compare its performance with WO_3 before making conclusion.

The crystal structure of spinel $Li_4Ti_5O_{12}$ belongs to the $Fd\bar{3}m$ space group (No. 227). Li and O ions occupy the tetrahedral 8*a* sites and the octahedral 32*e* sites, respectively. One-sixth of the octahedral 16*d* sites are randomly occupied by Li, while Ti fills in the remaining 5/6th. The structure can be described as $[Li_3]_{8a}[LiTi_5]_{16d}[O_{12}]_{32e}$. In order to satisfy the stoichiometry of $Li_4Ti_5O_{12}$, a $1 \times 1 \times 3$ supercell model is constructed to give the appropriate ratio of all elements. We adopt the structure found in the literature,[12,13] which has the lowest total energy per unit cell, out of many possibilities.

We perform spin-polarized DFT calculations,[14,15] as implemented in the Vienna *ab initio* Simulation Package (VASP),[16,17] using generalized gradient approximation (GGA) parameterized by Perdew-Burke-Ernzerhof (PBE).[18] The interaction potentials of the core electrons were replaced by projector augmented wave (PAW)[19] pseudopotentials (Li_sv, Ti_pv, O). All calculations employed a 600 eV cutoff energy for the plane wave basis.

For structure relaxation, k-point sampling was done on a $3 \times 3 \times 1$ Γ centered Monkhorst-Pack grid, with a small broadening width of Gaussian smearing (0.05 eV). The energy difference and force required for convergence were set to 10^{-6} eV and 0.01 eV/Å, respectively, which achieved a reasonable balance between accuracy and numerical cost. All atoms were fully relaxed to simulate the optimized structure of each lattice model. For optical property calculations, the number of bands was tripled, compared to the ground state. As Ti-3d states have strong on-site Coulomb interaction of localized electrons, DFT+U corrections were introduced with $U = 2.5$ eV to overcome shortcomings of PBE in structure relaxation and optical property calculations.[20,21]

To better understand the bandgap of LTO, we carried out Heyd-Scuseria-Ernzerhof (HSE06) hybrid functional calculations in the density of states (DOS),[22–25] with the k-space sampled only by the Γ point. HSE06 is generally better at predicting energy gaps but is significantly more costly than PBE+U, which meant we could not use it for all applications. The results from PBE+U were in generally good agreement with HSE06, supporting its use for other calculations. The details are provided in the supplementary material.

The highly contrasting optical behavior of $Li_4Ti_5O_{12}$ and $Li_7Ti_5O_{12}$ is the macroscopic performance of the electronic structure. Figure 1 reports the DOS and partial DOS results. $Li_4Ti_5O_{12}$ is a semiconductor with a calculated bandgap of 3.93 eV (HSE06), slightly larger than results (3.87 eV and 3.73 eV) in the literature.[26,27]

The charging process from $Li_4Ti_5O_{12}$ to $Li_7Ti_5O_{12}$ involves Li intercalating into LTO. The Li atom can easily lose an electron, forming a positive electric center and an additional electron. As the electronegativity of Ti (1.54) is larger than that of Li (0.98), this excess electron is more likely to be captured by Ti and occupy the d_{xy} orbit, which lifts the Fermi level and forms donor states next to the conduction band (CB), revealed by the peak in the bandgap in Fig. 1. The electrons in the d_{xy} orbit are weakly bounded by Ti, and so they have larger probability to overcome the donor ionization energy, entering the CB to be free electrons. This kind of impurity excitation is much easier than intrinsic excitation, which excites electrons in the valence band (VB) to the CB directly. That is why the absorption coefficient in the infrared region is greatly increased after charging. With more intercalated Li, the gap between VB and donor states narrows down to 2.39 eV, while the gap between donor states and CB and width of donor states expand to 0.67 and 1.28 eV, respectively. As a result, visible light (VIS) photons with the energy of 0.67–1.95 eV and above 2.39 eV will be absorbed by lithiated LTO, which means high transmittance from 519 nm to 636 nm (in accordance with Fig. 2). The actual light absorption process is more complicated, involving the coupling of phonons and photons, leading to lower transmittance in this wavelength range.

According to Maxwell's equations, the relationship between conductivity (σ) and absorption coefficient (α) is shown in the supplementary material. For a poorly conductive material (ω, angular frequency, $\omega \rightarrow 0$), the absorption coefficient (α) is nearly zero. However, for good conductive materials, the absorption coefficient (α) can be very large,

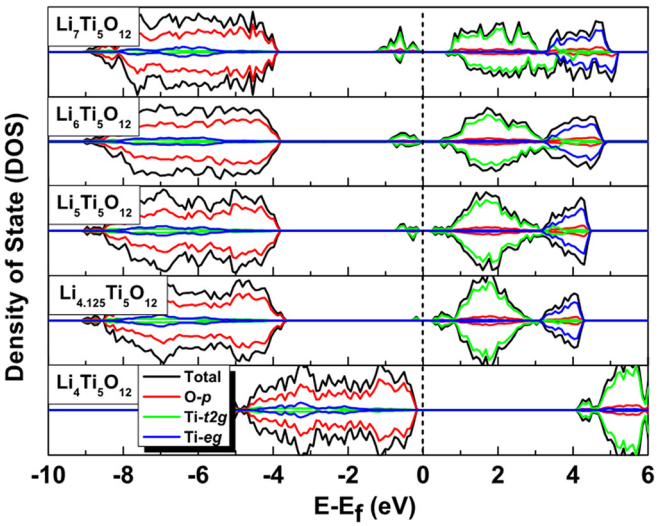

FIG. 1. Total and projected DOS. The Fermi level is aligned to zero.

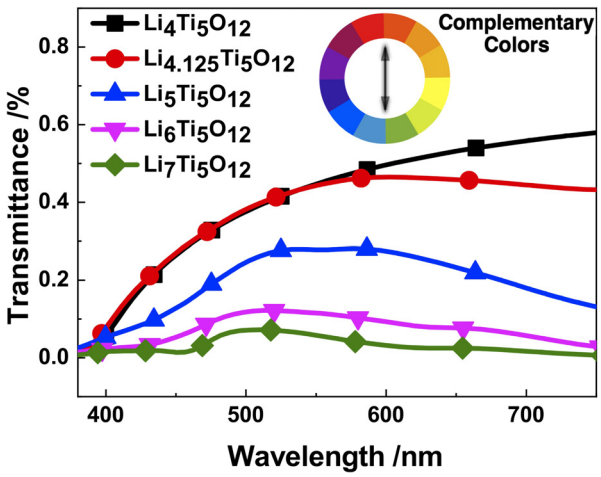

FIG. 2. The transmittance of LTO in visible light.

$$\alpha \approx \sqrt{2\mu_0\omega\sigma} \quad \left[\text{when } \frac{\sigma}{\mu\varepsilon\varepsilon_0\omega} \gg 1\right], \tag{1}$$

where ε is the permittivity and μ the permeability of the material; ε_0 is the permittivity of free space and μ_0 the permeability of free space.

As a result, due to the appearance of the donor states, the energy required to excite electrons into the CB is lower (both impurity excitation and intrinsic excitation). So the conductivity is improved, and the absorption coefficient is enhanced according to Eq. (1). Specific electronic information in the DOS graph and charge population analysis can be found in the supplementary material.

We now turn to optical theory. Light radiation falling onto a material will be reflected, absorbed, and transmitted (Fig. S2). The material's transmittance (T), absorbance (A), and reflectance (R) are then subject to the equation:[28] $T(\lambda) + A(\lambda) + R(\lambda) = I_0$. According to the Beer-Lambert law (α: absorption; x: thickness): $A(\lambda) = I_0(1 - e^{-\alpha x})$, absorption is zero at the upper surface ($x = 0$) of a material. Here, the vertical incident light intensity is I_0. Following is the specific properties of LTO.

In visible light, the change in reflectivity from $Li_4Ti_5O_{12}$ to $Li_7Ti_5O_{12}$ is negligible (Fig. S3). The increase in the absorption coefficient is extremely substantial, however. As a result, the transmittance (Fig. 2) is gradually lowered, and the color deepens, which can be calculated by integrating the transmitted energy (T) in sunlight ($\lambda_1 = 400$ nm and $\lambda_2 = 700$ nm),

$$T = \frac{\sum_{\lambda_1}^{\lambda_2} T(\lambda) S_\lambda \Delta\lambda}{\sum_{\lambda_1}^{\lambda_2} S_\lambda \Delta\lambda}, \tag{2}$$

where S_λ is the relative spectral distribution of solar radiation, $T(\lambda)$ is spectral transmittance of LTO, and λ is the wavelength. According to Fig. 2 and the solar spectrum at the Earth's surface,[29] the transmitted energy of sunlight of different colors through a 5 μm thick LTO is listed in Table I. After intercalation with a small amount of Li to form $Li_{4.125}Ti_5O_{12}$, LTO absorbs more light at the wavelength of 600–700 nm, corresponding to the red-orange color. Because of the redshift caused by the underestimated bandgap using the PBE method, the red and orange light will actually be absorbed more in $Li_{4.125}Ti_5O_{12}$ (T(lithiated)). Therefore, LTO shows the corresponding complementary color (the color wheel in Fig. 2), a mixture of blue and green.

TABLE I. Transmitted energy of sunlight of different colors for delithiated/lithiated ($Li_4Ti_5O_{12}/Li_{4.125}Ti_5O_{12}$) LTO (T: Transmitted energy, W/m^2).

Wavelength/nm	T(delithiated)	T(lithiated)	ΔT
380–450 (Violet)	8.97	9.68	+0.71
450–495 (Blue)	18.96	19.24	+0.28
495–570 (Green)	42.65	42.62	−0.03
570–590 (Yellow)	12.75	12.29	−0.46
590–620 (Orange)	19.73	18.34	−1.39
620–750 (Red)	84.47	69.27	−15.20

From Fig. 2, the more the Li intercalated in LTO, the higher the absorption and the lower the transmittance. Using Eq. (2) and the Air Mass 1.5 solar spectrum in the visible region, the transmitted energy for $Li_4Ti_5O_{12}$ accounts for 41.7% of total energy of visible light. By contrast, the value for $Li_7Ti_5O_{12}$ is only 3.8%, which makes it impossible for visible light to transfer through $Li_7Ti_5O_{12}$ and makes it appear black. Considering that the secondary and multiple reflections from the interface (LTO/air) within the LTO material can increase transmittance, especially for the material with a low absorption coefficient ($Li_4Ti_5O_{12}$), the range of adjustable light transmittance is likely to be larger than calculated. This theoretical result is in good agreement with reported experimental transmittance.[30,31]

Quantitative results of transmitted solar energy of different wavelengths are shown in Fig. 3, using Eq. (2) in the range of infrared (IR), visible light (VIS), and ultraviolet (UV). After charging to $Li_{4.125}Ti_5O_{12}$ from $Li_4Ti_5O_{12}$, the energy of transmitted VIS decreases only 1%, while transmitted IR shows a more substantial drop from 35% to 21%.

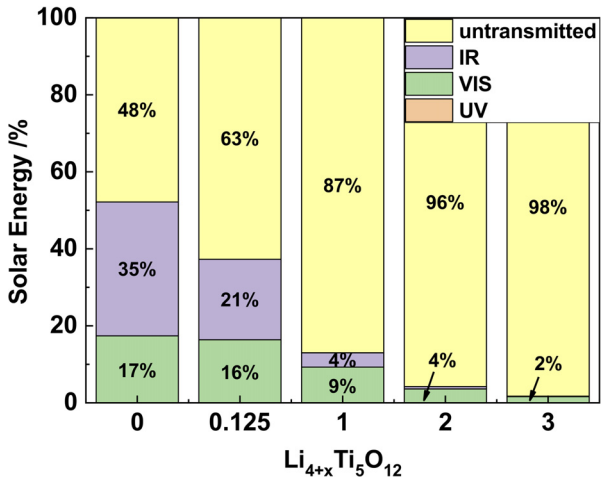

FIG. 3. Transmitted solar energy through a 5 μm thick LTO. 100% corresponds to the total energy of the AM 1.5 solar spectrum. UV contributions are essentially zero (maximum 0.06%) in all cases (VIS, 0.4–0.7 μm; IR, 0.7–2.75 μm; UV, 0.01–0.4 μm).

The difference will be more noticeable when charged to $Li_5Ti_5O_{12}$, which means that the absorption of infrared is highly sensitive to the intercalation of Li and even a small amount can significantly reduce transmittance of IR while maintaining transmittance of VIS.

The reflectivity and absorption coefficient of LTO in the same wavelength of the solar spectrum [Figs. 4(a) and 4(b)] are increased in general during lithiation, although the reflectivity coefficient is slightly reduced in the wavelength of 0.25–1.5 μm. Compared to the mild increase in the reflectivity coefficient, the absorption coefficient has increased by four orders of magnitude, which makes $Li_4Ti_5O_{12}$ change from an infrared transmission material to an infrared absorption material. The calculated transmittance of a 5 μm thick LTO is shown in Fig. 4(c), with the integrated transmittance between 63% and 0.2%. More importantly, consistent with the results in Fig. 3, the transmittance of $Li_{4.125}Ti5O_{12}$, which is intercalated with a small amount of Li, has a rapid decrease in the infrared range.

In the infrared range with a longer wavelength (3–15 μm), both reflection and absorption coefficients increase as x increases in $Li_{4+x}Ti_5O_{12}$ ($0 \leq x \leq 3$). There are two crucial infrared atmosphere windows, 3–5 μm and 8–14 μm, which are the operating wavelength ranges of infrared detection equipment and are denoted in light yellow in Figs. 4(d) and 4(e). The transmittance curve in Fig. 4(f) shows good adjustable performance in these two windows, from 70% to nearly 0% as x increases in $Li_{4+x}Ti_5O_{12}$. As a result, LTO can "appear" or "disappear" in infrared detection equipment by an applied voltage, analogous to previously reported behavior in WO_3.[33]

With the mechanism and properties mentioned above, LTO can be used in a wide range of applications in the electrochromic area.

In the visible light region, the electrochromic performance of LTO is remarkable since a single active LTO layer can achieve a transmittance range of 3.8%–41.7%, which has commercial potential in practical applications.

In the solar spectrum, on one hand, LTO has a transmittance range of 0.2%–63%. Considering infrared accounts for 52% to 55% of the energy of sunlight at Earth's surface and infrared has a significant thermal effect, the electrochromic properties of LTO can be effectively used to tune the transmission of infrared radiation, which allows the application of LTO in thermal management. On the other hand, the absorption coefficient of LTO in infrared is much more sensitive than in visible light. Such infrared absorption selectivity implies that when used as smart windows for buildings, the heat transmission and brightness can be controlled separately to a large extent. In contrast, WO_3, the most frequently used inorganic electrochromic material, has a high absorption coefficient in infrared under applied voltage, and therefore, the tunability is very limited. For example, LTO can lower heat transmission without significantly sacrificing brightness in summer and utilize the thermal effect of infrared in winter, which cannot be achieved by WO_3 due to its narrow bandgap. This can help reduce electricity consumption in buildings and thus the dependence on the cooling and heating system.

In mid- and long-wavelength infrared (MWIR and LWIR, 3–15 μm), the transmittance range of LTO is 0%–70%, making LTO an outstanding infrared camouflage material. In comparison, WO_3 has not been used for applications since the transmittance changes in this region are not significant.[11]

To conclude, this study reports DFT investigation of optical properties and DOS of the LTO material during the charging/

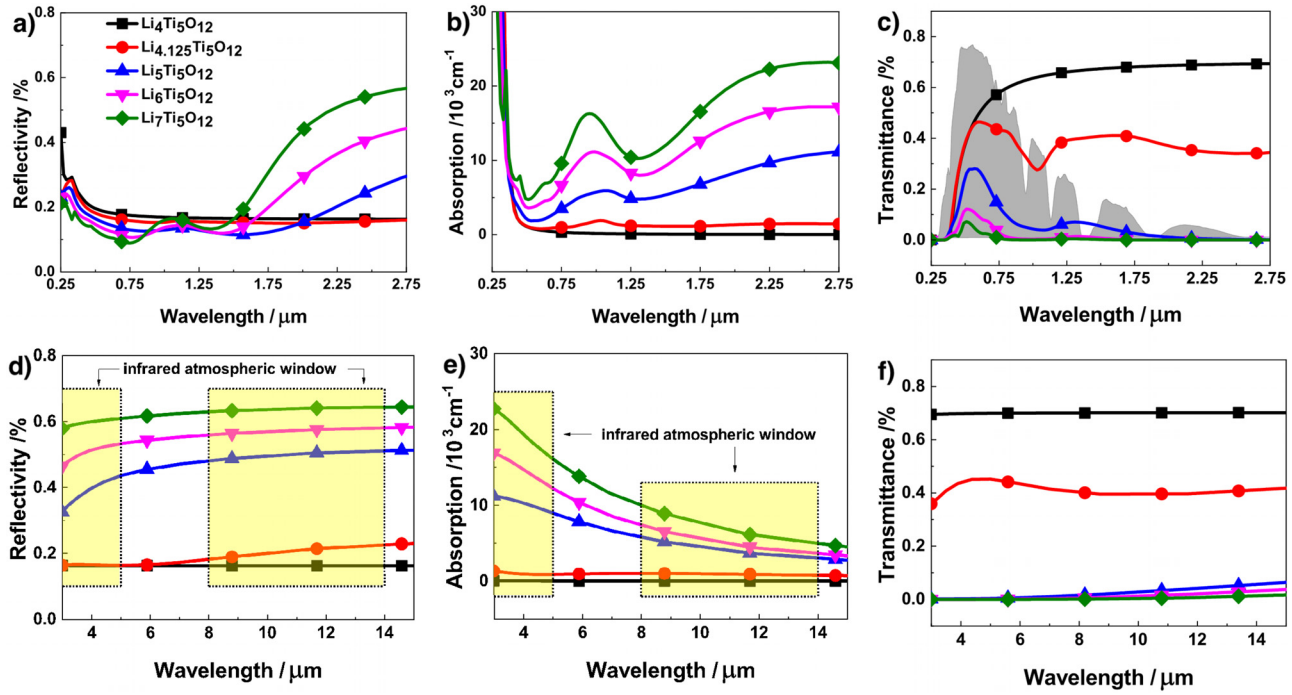

FIG. 4. (a), (b), and (c) are the reflectivity, absorption, and transmittance spectrum, and the gray area is the AM 1.5 solar spectrum.[29] (d), (e), and (f) are the reflectivity, absorption, and transmittance spectrum in midwavelength infrared (MWIR, 3–8 μm) and long-wavelength infrared (LWIR, 8–15 μm).[32]

discharging process. The results reported here theoretically demonstrate that $Li_4Ti_5O_{12}$ has excellent properties as a broadband electrochromic material for optical and thermal management. The mechanism behind it is the donor states in the forbidden band. Other methods which facilitate the formation of donor states can make similar changes to the electronic structure, including positive ion interstitial, higher-valence cation replacement, and negative ion vacancy.[9,34] These methods can be used to change the range of variations of the absorption coefficient and thereby tune the range of thermal transmittance. We recommend a thorough experimental study of the optical properties of LTO subject to these variations, as the theoretical properties uncovered in this work suggest that it is a promising material for more extensive applications in future smart windows.

See the supplementary material for more details and analysis about the DOS graph and electron population.

We wish to acknowledge the support of ARC Discovery from the Australian Research Council (No. DP170103721) and Soft Science Research Project of Guangdong Province (No. 2017B030301013).

REFERENCES

[1]S. K. Deb, "A novel electrophotographic system," Appl. Opt. **8**, 192–195 (1969).
[2]R. J. Mortimer, D. R. Rosseinsky, and P. M. S. Monk, *Electrochromic Materials and Devices* (Wiley, 2015).
[3]C. Granqvist, *Handbook of Inorganic Electrochromic Materials* (Elsevier Science, 1995).
[4]G. Qian and Z. Y. Wang, "Near-infrared organic compounds and emerging applications," Chemistry - An Asian Journal **5**, 1006–1029 (2010).
[5]L. Xiao, H. Ma, J. Liu, W. Zhao, Y. Jia, Q. Zhao, K. Liu, Y. Wu, Y. Wei, S. Fan, and K. Jiang, "Fast adaptive thermal camouflage based on flexible VO_2/graphene/CNT thin films," Nano Lett. **15**, 8365–8370 (2015).
[6]R. Mortimer and N. Rowley, "9.13-Metal complexes as dyes for optical data storage and electrochromic materials," in *Comprehensive Coordination Chemistry II*, edited by J. A. McCleverty and T. J. Meyer (Pergamon, Oxford, 2003), pp. 581–619.
[7]T. Xu, E. C. Walter, A. Agrawal, C. Bohn, J. Velmurugan, W. Zhu, H. J. Lezec, and A. A. Talin, "High-contrast and fast electrochromic switching enabled by plasmonics," Nat. Commun. **7**, 10479 (2016).
[8]H. Demiryont and D. Moorehead, "Electrochromic emissivity modulator for spacecraft thermal management," Sol. Energy Mater. Sol. Cells **93**, 2075–2078 (2009).
[9]J. Qiu, C. Lai, E. Gray, S. Li, S. Qiu, E. Strounina, C. Sun, H. Zhao, and S. Zhang, "Blue hydrogenated lithium titanate as a high-rate anode material for lithium-ion batteries," J. Mater. Chem. A **2**, 6353–6358 (2014).
[10]X. Yu, R. Wang, Y. He, Y. Hu, H. Li, and X. Huang, "Electrochromic behavior of transparent $Li_4Ti_5O_{12}$/FTO electrode," Electrochem. Solid-State Lett. **13**, J99–J101 (2010).
[11]J. Mandal, S. Du, M. Dontigny, K. Zaghib, N. Yu, and Y. Yang, "$Li_4Ti_5O_{12}$: A visible-to-infrared broadband electrochromic material for optical and thermal management," Adv. Funct. Mater. **28**, 1802180 (2018).
[12]P.-C. Tsai, W.-D. Hsu, and S.-K. Lin, "Atomistic structure and ab initio electrochemical properties of $Li_4Ti_5O_{12}$ defect spinel for Li ion batteries," J. Electrochem. Soc. **161**, A439–A444 (2014).
[13]S. Zahn, J. Janek, and D. Mollenhauer, "A simple ansatz to predict the structure of $Li_4Ti_5O_{12}$," J. Electrochem. Soc. **164**, A221–A225 (2017).
[14]P. Hohenberg and W. Kohn, "Inhomogeneous electron gas," Phys. Rev. **136**, B864–B871 (1964).
[15]W. Kohn and L. J. Sham, "Self-consistent equations including exchange and correlation effects," Phys. Rev. **140**, A1133–A1138 (1965).
[16]G. Kresse and J. Furthmüller, "Efficiency of ab-initio total energy calculations for metals and semiconductors using a plane-wave basis set," Comput. Mater. Sci. **6**, 15–50 (1996).
[17]G. Kresse and J. Furthmüller, "Efficient iterative schemes for ab initio total-energy calculations using a plane-wave basis set," Phys. Rev. B **54**, 11169–11186 (1996).
[18]J. P. Perdew, K. Burke, and M. Ernzerhof, "Generalized gradient approximation made simple," Phys. Rev. Lett. **77**, 3865–3868 (1996).
[19]P. E. Blöchl, "Projector augmented-wave method," Phys. Rev. B **50**, 17953–17979 (1994).
[20]Y. Gao, Z. Wang, and L. Chen, "Stability of spinel $Li_4Ti_5O_{12}$ in air," J. Power Sources **245**, 684–690 (2014).
[21]Z. Hu and H. Metiu, "Choice of U for DFT+U calculations for titanium oxides," J. Phys. Chem. C **115**, 5841–5845 (2011).
[22]J. Heyd, G. E. Scuseria, and M. Ernzerhof, "Hybrid functionals based on a screened Coulomb potential," J. Chem. Phys. **118**, 8207–8215 (2003).
[23]J. Heyd, G. E. Scuseria, and M. Ernzerhof, "Erratum: 'Hybrid functionals based on a screened Coulomb potential' [J. Chem. Phys. **118**, 8207 (2003)]," J. Chem. Phys. **124**, 219906 (2006).
[24]A. V. Krukau, O. A. Vydrov, A. F. Izmaylov, and G. E. Scuseria, "Influence of the exchange screening parameter on the performance of screened hybrid functionals," J. Chem. Phys. **125**, 224106 (2006).
[25]J. Paier, M. Marsman, K. Hummer, G. Kresse, I. C. Gerber, and J. G. Ángyán, "Screened hybrid density functionals applied to solids," J. Chem. Phys. **124**, 154709 (2006).
[26]M. G. Verde, L. Baggetto, N. Balke, G. M. Veith, J. K. Seo, Z. Wang, and Y. S. Meng, "Elucidating the phase transformation of $Li_4Ti_5O_{12}$ lithiation at the nanoscale," ACS Nano **10**, 4312–4321 (2016).
[27]H. Song, S.-W. Yun, H.-H. Chun, M.-G. Kim, K. Y. Chung, H. S. Kim, B. W. Cho, and Y.-T. Kim, "Anomalous decrease in structural disorder due to charge redistribution in Cr-doped $Li_4Ti_5O_{12}$ negative-electrode materials for high-rate Li-ion batteries," Energy Environ. Sci. **5**, 9903–9913 (2012).
[28]B. P. Jelle, "Solar radiation glazing factors for window panes, glass structures and electrochromic windows in buildings—Measurement and calculation," Sol. Energy Mater. Sol. Cells **116**, 291–323 (2013).
[29]See https://www.nrel.gov/grid/solar-resource/spectra-am1.5.html for "Reference Air Mass 1.5 Spectra."
[30]M. Roeder, A. B. Beleke, U. Guntow, J. Buensow, A. Guerfi, U. Posset, H. Lorrmann, K. Zaghib, and G. Sextl, "$Li_4Ti_5O_{12}$ and $LiMn_2O_4$ thin-film electrodes on transparent conducting oxides for all-solid-state and electrochromic applications," J. Power Sources **301**, 35–40 (2016).
[31]S. Scharner, W. Weppner, and P. S. Beurmann, "Evidence of two-phase formation upon lithium insertion into the $Li_{1.33}Ti_{1.67}O_4$ spinel," J. Electrochem. Soc. **146**, 857–861 (1999).
[32]J. Byrnes, *Unexploded Ordnance Detection and Mitigation* (Springer, Netherlands, 2008).
[33]K. Sauvet, L. Sauques, and A. Rougier, "IR electrochromic WO_3 thin films: From optimization to devices," Sol. Energy Mater. Sol. Cells **93**, 2045–2049 (2009).
[34]X. Chen, L. Liu, P. Y. Yu, and S. S. Mao, "Increasing solar absorption for photocatalysis with black hydrogenated titanium dioxide nanocrystals," Science **331**, 746–750 (2011).